Synergistic-Functional-Structural Resolution Recovery Algorithm

Initially, both functional and structural images are decomposed trough the Dual Tree Complex Wavelet Transform DT-CWT (1) into several resolution elements. The estimated wavelet coefficients are then collected into two separate matrixes $W_{PET,j}$ (as derived from the original PET image) and $W_{SR,j}$ (as derived from the structural reference image) for each resolution level j. In this implementation we set $j = 1,2$ meaning that two consecutive wavelet decompositions are to the same original image.

The high-resolution coefficients of the functional decomposition are then "replaced" with the coefficients of the structural one by means of combining the two matrices with appropriate local scaling as follows

$$W_{PET,j}^{new} = \text{scaling}_1 \cdot W_{SR,j} + \text{scaling}_2 \cdot W_{PET,j} \quad \text{[eq1.a]}$$

$$W_{PET,j}^{new}(q,k) = R_j \cdot \{G_j \cdot \gamma_j(q) \cdot W_{SR,j}(q,k) + [1 - \gamma_j(q)] \cdot W_{PET,j}(q,k)\} \quad \text{[eq1.b]}$$

where $q \in Q$ indexes the number of quadrants in the wavelet decomposition and k the position in the wavelet domain within each quadrant.

The $W_{PET,j}^{new}$ coefficients are then back-projected into image space using the inverse DT-CWT to obtain the new high-resolution functional image

In Eq. 1.b R_j is the recovery coefficient accounting for the difference in resolution between the functional and anatomical images and is defined as

$$R_j = \frac{\sum_k \sum_q W_{SR,j}(q,k)}{\sum_k \sum_q W_{SR,j}(q,k)} \quad [2]$$

where W_{SR_s} s is the wavelet transform of the structural reference image smoothed with a 3D Gaussian filter to match the PET scanner resolution (a FWHM of 4mm was selected following a simulation study).

G_j is the anatomical-to-functional global calibration factor and is defined as

$$G_j = \frac{\sum_k \sum_q W_{PET,j}(q,k)}{\sum_k \sum_q W_{SR,j}(q,k)} \quad [3]$$

The branching ratio γ_j weights the anatomical information by taking into account anatomical variability and statistical variability through measures of wavelet quadrants variance

$$\gamma_j(q) = \frac{SSW_j(q)}{SSW_j(q) + SSB_j} \quad [4]$$

Note that in Eq. 4 the between quadrant variance SSB depends on anatomical variability while the within quadrant variance SSW is mainly due to stochastic fluctuation and are defined as

$$SSB_j = Q \cdot \sum_k \left(\frac{\sum_q W_{PET,j}}{Q} - \frac{\sum_k \sum_q W_{PET,j}}{Q \cdot K} \right)^2 \quad [5]$$

$$SSW_j(q) = \sum_k \left(W_{PET,j} - \frac{\sum_q W_{PET,j}}{Q} \right)^2 \quad [6]$$

When the functional image contains enough structural information the *SSB* will overtake the *SSW* reducing the amount of structural input in Eq. 1.b due to a smaller branching ratio γ_j.

In contrast to the original work of Shidahara et al (2) the branching ratio γ_j is calculated taking into consideration each quadrant in wavelet domain separately instead of averaging over the diagonal ones only.

The rationale behind this choice depends on the nature of PET image noise that, being non-white and correlated, projects differently into each wavelet quadrant (3) Therefore accurate estimation of the variance of the wavelet coefficients requires independent computation in each quadrant.

References

1. Kingsbury N. Complex wavelets for shift invariant analysis and filtering of signals. *Applied and computational harmonic analysis.* 2001;10:234-253.

2. Shidahara M, Tsoumpas C, Hammers A, et al. Functional and structural synergy for resolution recovery and partial volume correction in brain PET. *Neuroimage.* 2009;44:340-348.

3. Turkheimer FE, Brett M, Visvikis D, Cunningham VJ. Multiresolution analysis of emission tomography images in the wavelet domain. *Journal of Cerebral Blood Flow & Metabolism.* 1999;19:1189-1208.

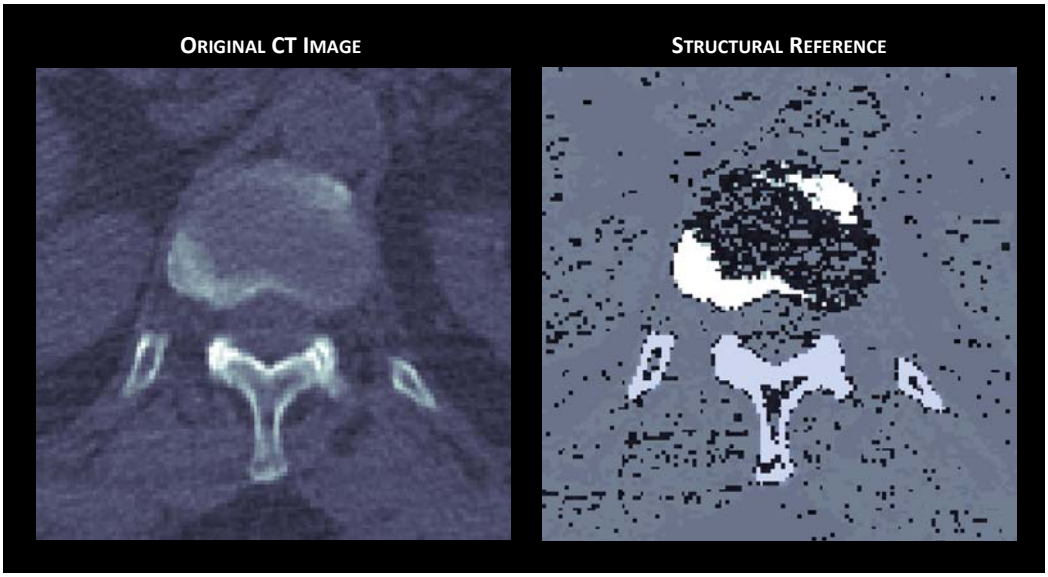

SUPPLEMENTAL FIGURE 1. Comparison between original CT image (left) and structural reference image (right) for a zoomed transaxial spinal view. The ROIs of the structural reference are defined by automatic thresholding the original CT intensities in Hounsfield Units; the new value for each ROI is defined as the average activity of each corresponding region in the original PET image.

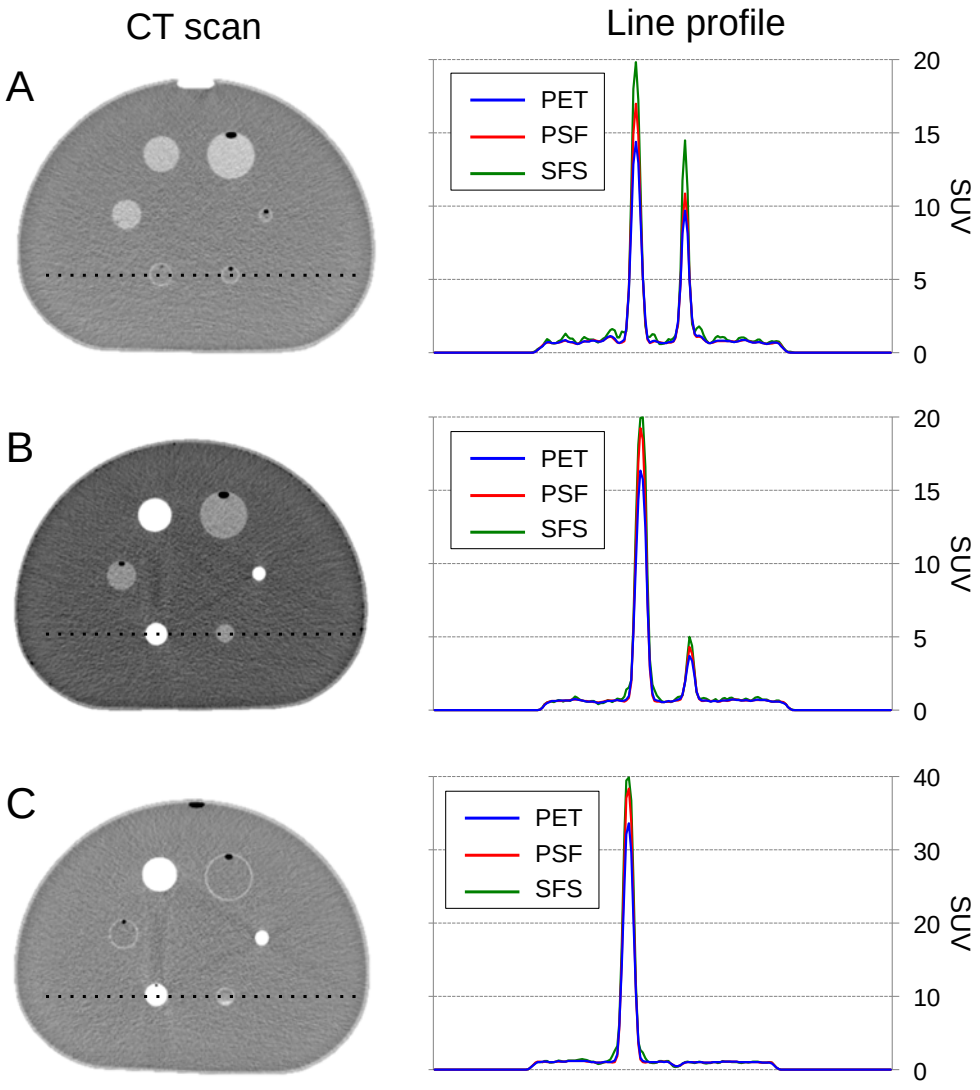

SUPPLEMENTAL FIGURE 2. CT images and line profiles of three different phantom experiment acquisitions (one for each line).

The line profiles in the 2nd column refer to the position highlighted by the dashed line on the CT. The line profiles are reported for all the three imaging modalities under examination: standard PET (blue line), PET-PSF (red line) and PET-SFS (green line).

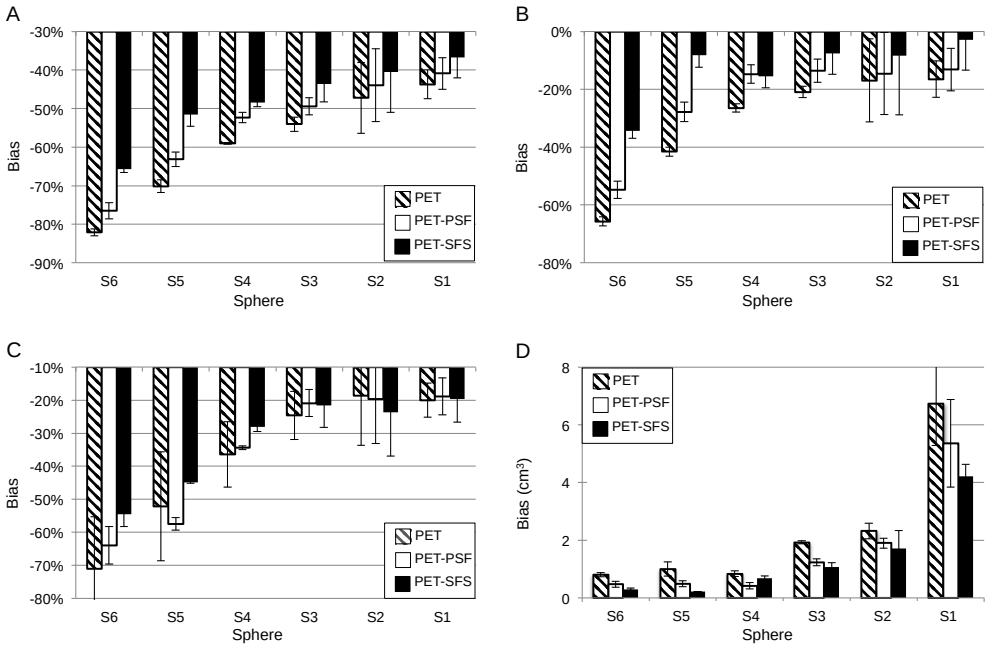

SUPPLEMENTAL FIGURE 3. Activity quantification and MATV estimates bias obtained as an average among the three phantom experiments. A-C) comparison of percentage differences from ground truth in A) SUV_{mean}, B) SUV_{max} and C) SUV_{peak}; D) comparison of absolute differences from ground truth in sphere MATV estimates (x-axis sphere are in reverse order compared to a-c). Bias comparison of images obtained with different modalities: standard PET (dark gray bar), PET with PSF reconstruction (light grey bar) and PET corrected with SFS-RR algorithm (black bar).

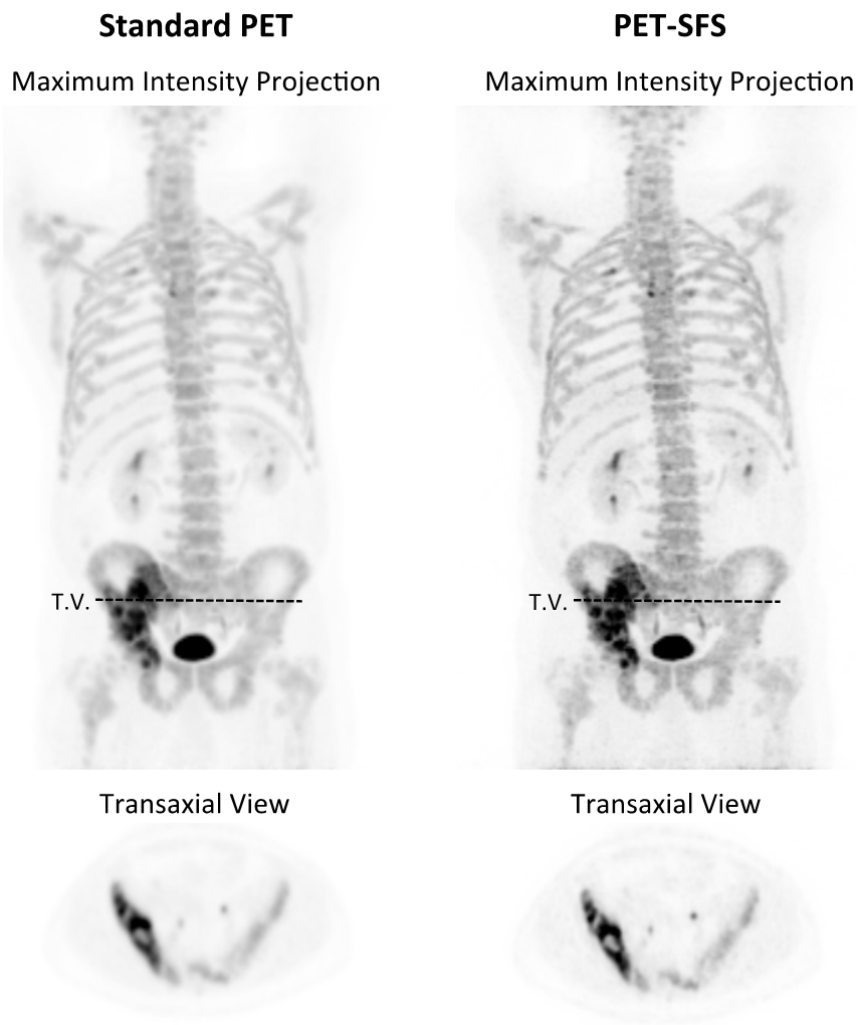

SUPPLEMENTAL FIGURE 4. Upper Panels Maximum Intensity Projection (MIP) view of Patient02. Lower Panels Transaxial view corresponding to the dashed line reported on the MIP. Left Panels Standard PET; Right Panels PET corrected with SFS-RR algorithm.

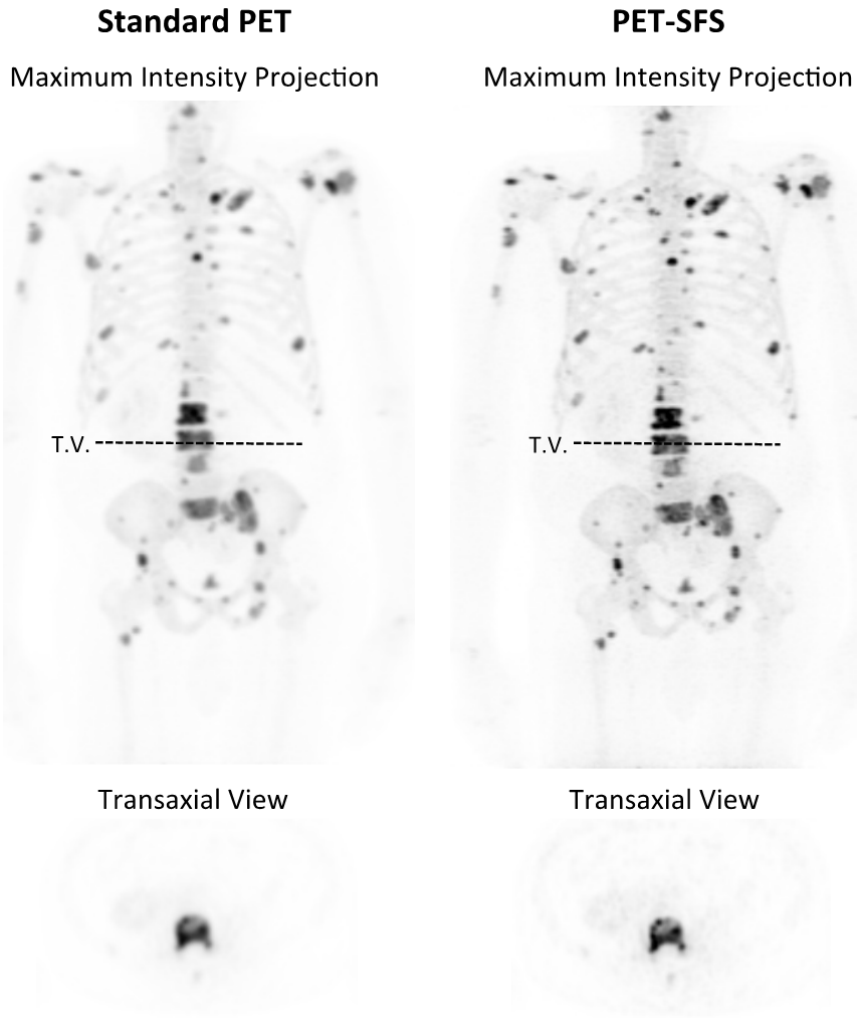

SUPPLEMENTAL FIGURE 5. Upper Panels Maximum Intensity Projection (MIP) view of Patient03. Lower Panels Transaxial view corresponding to the dashed line reported on the MIP. Left Panels Standard PET; Right Panels PET corrected with SFS-RR algorithm.

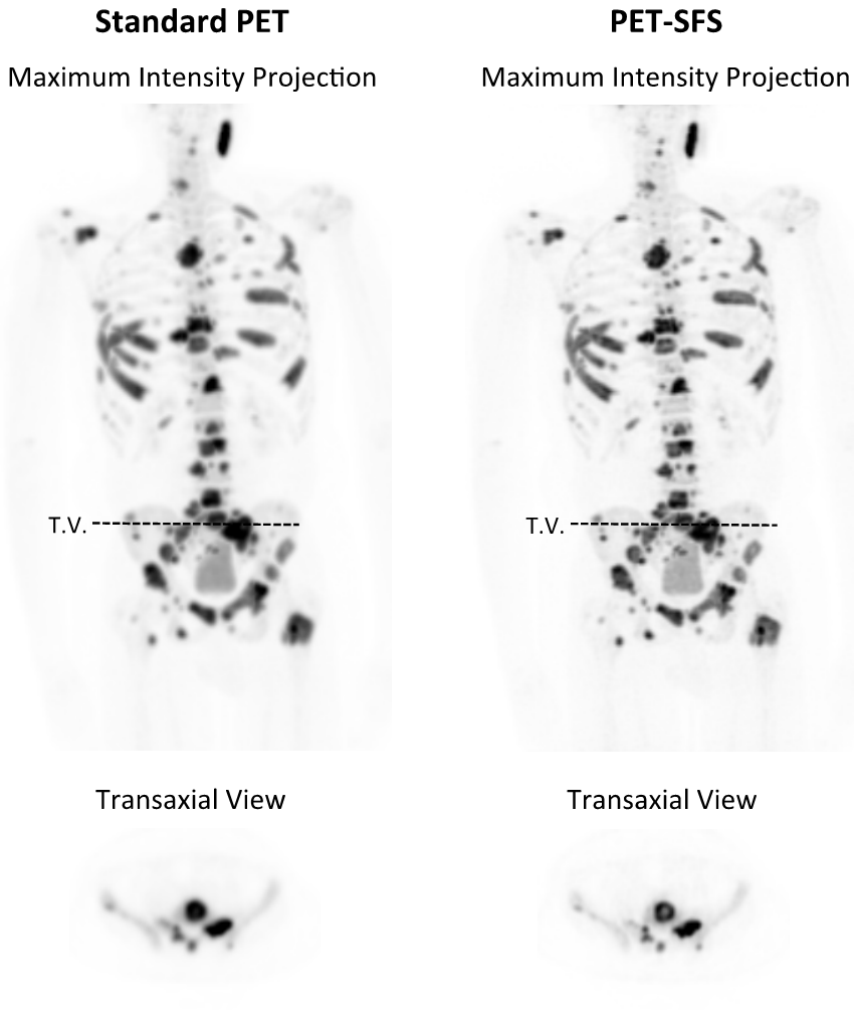

SUPPLEMENTAL FIGURE 6. Upper Panels Maximum Intensity Projection (MIP) view of Patient04. Lower Panels Transaxial view corresponding to the dashed line reported on the MIP. Left Panels Standard PET; Right Panels PET corrected with SFS-RR algorithm.

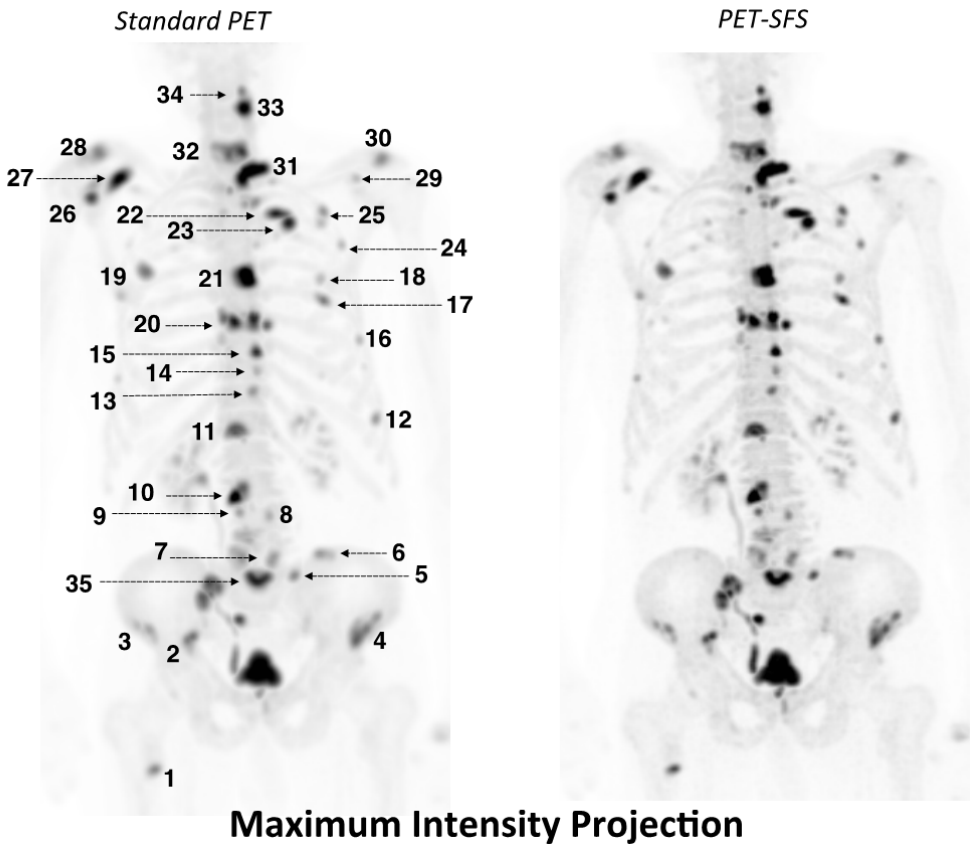

SUPPLEMENTAL FIGURE 7. Maximum Intensity Projection view of Patient01. Left Panel Standard PET; Right Panel PET corrected with SFS-RR algorithm.

Lesions indexes are also reported (right panel). Corresponding SUVs and volumes estimates are reported in Supplemental Table 1.

SUPPLEMTENTAL TABLE 1 –Patient01

	SUVmean		**SUVmax**		**SUVpeak**		**MATV [cm³]**	
Lesion	PET	PET-SFS	PET	PET-SFS	PET	PET-SFS	PET	PET-SFS
1	14.41	25.59	29.10	48.73	19.62	30.62	2.69	1.27
2	10.10	15.06	22.27	32.60	15.42	19.28	9.56	4.69
3	17.78	27.43	35.33	57.45	25.05	31.96	5.50	2.93
4	19.25	20.52	38.88	33.91	30.54	25.63	12.08	8.36
5	15.00	26.24	30.57	52.00	20.78	30.27	2.08	1.03
6	12.36	19.56	23.68	39.81	17.62	23.18	4.01	2.25
7	15.01	25.81	30.57	52.00	19.20	25.79	2.18	1.08
8	8.32	11.68	19.30	19.53	13.48	13.43	5.77	2.27
9	11.45	21.84	23.92	44.20	16.80	31.39	2.74	1.30
10	37.16	52.24	76.45	106.60	54.62	72.46	5.18	3.91
11	23.16	33.08	41.12	62.92	33.91	39.38	7.53	5.18
12	13.15	23.71	25.31	45.33	14.73	27.55	1.78	1.25
13	9.63	14.67	16.42	24.43	13.19	17.76	4.77	2.18
14	9.31	10.75	18.70	15.60	14.62	12.93	4.89	3.15
15	26.64	45.22	55.17	89.25	34.76	63.11	2.79	1.59
16	9.14	18.05	17.44	34.60	11.86	20.46	1.49	1.00
17	17.37	31.21	32.78	60.82	21.43	34.00	1.88	1.17
18	9.25	16.47	17.78	32.12	11.61	18.11	1.71	1.12
19	17.96	25.50	33.77	47.35	23.99	30.34	3.77	2.81
20	28.46	38.51	59.49	68.29	42.15	44.05	11.61	6.92
21	47.53	60.96	88.69	115.52	75.39	84.73	6.77	5.40
22	30.68	49.04	59.11	100.23	42.74	63.77	2.76	2.05
23	29.80	42.89	58.43	83.39	41.35	54.07	3.11	2.18
24	8.64	17.37	16.90	32.91	12.69	21.53	1.56	1.23
25	12.03	20.67	25.04	43.14	16.31	26.78	3.99	2.00
26	22.88	35.25	46.60	67.20	33.73	43.63	3.99	1.96
27	35.20	44.25	67.93	83.17	52.46	62.85	5.65	4.55
28	14.90	17.25	30.28	36.10	24.44	27.69	9.63	8.09
29	7.65	15.24	16.89	29.83	11.26	16.18	3.13	1.00
30	13.79	16.95	27.25	34.19	21.34	24.89	6.23	4.87
31	43.74	58.49	81.85	106.39	66.42	77.64	9.19	6.65
32	24.07	31.98	48.69	67.02	37.60	44.50	12.59	8.36
33	36.75	47.41	69.06	85.36	54.23	66.19	4.25	3.40
34	16.09	30.02	31.23	56.12	21.37	38.67	1.76	1.05
35	29.73	40.90	56.80	79.30	44.63	52.91	7.31	5.01

Standardized Uptake Values (SUV_{mean}, SUV_{max}, SUV_{peak}) and Metabolic Active Tumor Volume (MATV) estimates computed for all the lesions indexed in Figure 7 after automated segmentation. Values are

reported for estimates obtained from the standard PET and PET corrected with the SFS-RR algorithm images.